An idea of distributed parameter control for scramjet engines

Y. Daren, C. Tao and B. Wen
Harbin Institute of Technology
Heilongjiang, China

ABSTRACT

Scramjet engines are used under extreme temperatures and with wide range of Mach numbers from 3 to 8 or higher and have shown different control properties from other airbreathing engines. New control problems involving distributed parameter control have been found concerning investigations of the control of scramjet engines whose physical states are spatially interacted and whose governing equations are partial differential equations. The work of this paper is based on the application of distributed parameter control conception to study the control problems of scramjet engines with the aim of achieving the desirable design properties and increasing control reliability. A new control idea based on shape control theory is put forward to realise the distributed parameter control of scramjet engines with the preconditions of proper space dimension and frequency-domain simplification. Simulation results and theoretic analysis for an axisymmetric, wall-injection scramjet engine show the feasibility and validity of the control idea.

NOMENCLATURE

A	cross-sectional area
e	exergy
E	entropy waves
GM	gain margin
h	enthalpy
J	objective function
J^+	fast acoustic waves
J^-	slow acoustic waves
k	ratio of specific heats
M	Mach number
p	pressure
PM	phase margin
q	heat release
s	entropy
S	sensitivity
T	temperature
W	unmodelled dynamics
x	position co-ordinate along the axis of the channel
α	speed of sound
τ	stagnation temperature rise ratio
τ_p	propagation time
ω_0	shear frequency
$\xi\cdot$	damping coefficient

Subscripts

c	core flow
t	total
*	at the critical point

Paper No. 3142. Manuscript received 6 October 2006, revised 12 October 2007 accepted 16 October 2007.

https://doi.org/10.1017/S0001924000001901 Published online by Cambridge University Press

1.0 INTRODUCTION

Complex systems, such as aeronautic engines in aerospace, must be controlled in order to achieve designated missions or operational requirements[1]. Fuel control is one of the key technologies to a successful scramjet engine[2]. The fuel control system must effectively deal with varying inlet conditions and the combustion generated pressure rise must be controlled precisely to maximise engine performance without unstarting the inlet[3]. In order to meet this challenge, the fuel control system must inject the fuel so that its heat release profile will produce the required pressure rise at each Mach number. This pressure rise is a complex response to the inlet Mach number and the fuel state. At low Mach numbers, the pressure rise due to a given heat release is greater than that at higher Mach numbers; Unfortunately the inlet tolerance to pressure rise is generally less at low speeds. This requires the heat release to be further aft at low speeds than at higher speeds, and this ideal heat release location moves forward with flight speed. Compounding the designer's problem is the drastic changes in fuel density and reactivity. This changes the injection penetration, mixing and combustion rate at each Mach number[4]. The ideal combustor would have an infinite number of uniquely different injectors to keep the heat release profile in the ideal location for each speed[5]. This is impractical so fuel control shall play a more important role in providing the designated heat release profile, and then keeping the designated operational performance at each Mach number.

The critical problems of matching heat release profile to combustor shape over a wide speed range have early been proposed in 1970s when Ferri[6] created the concepts that tailor the aerothermodynamics of fuel injection, mixing, and diffusive combustion to the desired engineering features of the fixed geometry scramjet engines. But the challenges of engine design with assuring controlled heat release and avoiding strong inlet–combustor interactions, in a very demanding ground-test environment, make the timely achievement of such an undertaking very difficult indeed. Now these problems are still to some degree worrying the engine designers[7,8]. To help solving the problems of matching heat release profile to combustor shape, this paper makes some suggestions from a viewpoint of applying distributed parameter control technologies.

As known, all aeronautic engines in use are spread out in space and are distributed parameter systems governed by partial differential equations. But as viewed from the past or the present, lumped parameter control methods are mainly used[9]. There exist two reasons that the control systems of these distributed parameter systems are designed as lumped parameter plants. One is that it is sufficient to make a lumped model approximation by reasonable simplifications. The other is that lumped parameter control will have to be used because of the difficulties in applying distributed parameter control. However, it's hard to achieve the satisfactory performance on thrust level and operating safety. Scramjet engines are such systems with obvious distributed parameter properties characterised by complex scramjet combustion and inlet-combustor interactions along the flow field. The flow field in a scramjet engine is transitional over a wide speed range, and in this range engine performance is characterised by complex transitional fluid dynamics, supersonic/subsonic flows with corresponding shock fields, coupled heat release/shock generation, combustion thermodynamics and chemical reactions[10,11]. So there are benefits from thinking scramjet engines through in terms of continuum mechanics with distributed parameter control.

2.0 FUNDAMENTAL CONTROL PROBLEMS OF SCRAMJET ENGINES

Because scramjet engines are used under extreme temperatures and with wide range of Mach numbers, they show different control properties from other airbreathing engines, such as turbojet and ramjet engines.

2.1 Lumped parameter control problems of turbojet and ramjet engines

Some turbojet engines currently in production have yet used single-input single-output (SISO) controllers when having only fuel flow as the input variable and rotational speed as the output variable can have adequate controllers. For most modern turbojet engines with afterburners and variable geometry compressors operating in varied flight segments, a more complex control using multiple-input multiple-output (MIMO) techniques[12] has to be designed due to the strong interactions. The input variables include the main engine fuel flow and the nozzle area; variable geometry and afterburner fuel flow may also be the input variables in more complex engines. Parameters of interest for the controllers are the output variables. In order to use the important characteristics of the engines, the rotational speeds are selected as the output variable. Also other characteristic states variables can be taken such as the temperature and pressure of the intake, combustion chamber and compressor discharge[13]. These modern engines being multivariable in nature require more complicated control mechanisms and better control strategies for enhanced control over the variables to ensure improved performance of the plant[14]. Hence, new control techniques like linear feedback, optimal control, fuzzy control, sliding mode control etc. are being investigated in literatures.

Ramjet engines are characterised by normal shock compression instead of the rotating compressor components for the turbojet engines. The normal shock may be used to describe the compression performance of the ramjet engines' inlet as well as the rotational speed, therefore its position or pressure rate may be selected as the controlled output variable[15]. Ramjet engines are also characterized by constant cross-sectional area combustor profile with subsonic combustion. Therefore the impulse function is invariable along the combustor channel, then the aerodynamic parameters of the combustor are mainly determined by the heat release energy if the added fuel mass is neglected. Because subsonic combustion is of high combustion efficiency and total pressure recovery, the inlet and outlet parameters of the combustor are mainly determined by the total heat release energy almost regardless of the fuel distribution along the combustor channel. It is for these reasons that the total temperature at the outlet of the combustor or the Mach number at the inlet of the combustor may be selected as the controlled output variable[16].

As from the above discussions, control technologies for the turbojet and ramjet engines are still in the frame of lumped parameter control where characteristic states variables can be found and chosen to represent the distributed parameter nature of the system by ordinary differential equations instead of partial differential equations.

2.2 Distributed parameter control problems of scramjet engines

Because they are difficult to deal with, engineers generally avoid partial differential equations. It is desirable to represent the physical system by a simplified mathematical model which describes only the significant characteristics of the system behaviour. The control variables which have a major influence on the outputs and states are retained in the mathematical model; a lumped parameter control is then feasible[17]. But it's not certain for scramjet engines if lumped parameter control can achieve the designate performance for the complex spatial interaction of the supersonic flow and supersonic combustion where the spatial effects can not be neglected[10]. There are two problems primarily associated with scramjet engine control.

One is the enormous irreversible losses of supersonic combustion and shock system at high Mach number[18]. The incoming flow stagnation pressure irreversibly decreases as the flow passes through the bow shock and then the inlet shock system of the scramjet engine. At high Mach number, the flow throughout the combustor channel, by definition, is supersonic. Thus the combustor is appre-

https://doi.org/10.1017/S0001924000001901 Published online by Cambridge University Press

ciably longer than that in a turbojet or ramjet engine, with a significant amount of surface area resulting in skin friction and heat transfer. On a one-dimensional basis, the differential change in the stagnation pressure can be written as

$$\frac{1}{p_t}\frac{\mathrm{d}p_t}{\mathrm{d}x} = -\frac{k\mathrm{M}^2}{2}\frac{1}{T_t}\frac{\mathrm{d}T_t}{\mathrm{d}x} \quad \ldots (1)$$

where T_t is stagnation temperature. The overall change in is large because of the exothermic combustion process, and the overall skin friction is also large. Because the M^2 factor exceeds unity, the overall loss in stagnation pressure $p_{t\infty}$ in the combustor is amplified into a major loss. While the combustion loss of a turbojet or ramjet engine is much smaller because the M^2 factor is much less. These irreversible losses contribute to the low thrust level of scramjet engines at high Mach number. How to decrease the irreversible losses and achieve the designate performance becomes a more important problem compared to the turbojet or ramjet engines.

The other is the matching problem among inlet, combustor and nozzle over a wide speed range ($\mathrm{M}a3 \approx 8$)[19]. Scramjet engines are used over a wide speed range with combustion in the ramjet mode, transitional mode and scramjet mode respectively. As known, it is possible to design a perfect engine at a certain operating point, but its performance will drop rapidly without regulation once the operating point deviates greatly. Moreover, low matching performance among inlet, combustor and nozzle will even cause such serious safety problems as inlet unstart, flameout, etc.

From a viewpoint of control application, matching the heat release profile with the flow parameter distribution along the flow direction can help to decrease the irreversible losses of supersonic combustion and shock system at high Mach number, and better the matching performance among inlet, combustor and nozzle over a wide speed range. Applying exergy concepts to understand this idea, we get

$$e_x = (h_{tx} - h_{t\infty}) - \int_{\infty}^{x} T\mathrm{d}s + (\text{other terms}) = q_x \quad \ldots (2)$$

$$-\int_{\infty}^{x} T\mathrm{d}s + (\text{other terms}) = q_x$$

where the 'other terms' are used to denote exergy due to potential energy, chemical potential, radiation, heat transfer, etc. Note that exergy is mainly determined by the total heat release and entropy production (an integral effect). On a one-dimensional basis, the differential change of Mach number can be written as

$$\frac{\mathrm{dM}}{\mathrm{d}x} = \mathrm{M}\left(\frac{1+(k-1)\mathrm{M}^2/2}{1-\mathrm{M}^2}\right)\left\{-\left(\frac{1}{A_c}\frac{\mathrm{d}A_c}{\mathrm{d}x}\right)+\frac{1+k\mathrm{M}^2}{2}\left(\frac{1}{T_t}\frac{\mathrm{d}T_t}{\mathrm{d}x}\right)\right\} \quad \ldots (3)$$

Note that the Mach number distribution is mainly determined by the heat release profile for a fixed geometry scramjet engine. According to Equation (1), the stagnation pressure loss is also found to have an integral effect mainly determined by the heat release profile and Mach number distribution which are spatially interconnected.

As discussed above, spatial distribution of heat release and Mach number has a marked influence on the performance of the scramjet engine. With this understanding, properly regulating heat release profiles and Mach number distributions can decrease the integral of entropy production or stagnation pressure loss, better the matching performance, and thus increase the thrust level. This is a remarkable character of scramjet engines different from other airbreathing engines such as the turbojet and ramjet engines.

From the aerodynamics equations, the conception of regulating heat release profiles and Mach number distributions along the flow direction means regulating the flow parameter distribution by controlling the energy distribution (source terms), which belongs to a classic distributed parameter control conception.

3.0 PROPER SPACE DIMENSION FOR DISTRIBUTED PARAMETER CONTROL

The first problem for distributed parameter control is about space dimension. There are three kinds of choices for scramjet engines: zero space dimension, one space dimension and two or three space dimension.

The first choice is zero space dimension used in traditional lumped parameter control as an approximation to the original distributed parameter system. Approximation with zero space dimension is sufficient when there is good reason to believe the spatial variation can be neglected. But to the spatially interconnected systems of scramjet engines, it is difficult to acquire sufficient accuracy and reliability in describing the complex flow and combustion processes with so called low-order lumped parameter model. High-order lumped parameter model, however, will introduce such problems as difficulties in control system designs, complexities in control procedures, etc[20]. Moreover, the system will be uncontrollable when the number of state variables exceeds that of the control variables.

The second choice is one space dimension. Generally speaking, supersonic combustion is a chemical reaction process, accompanied by orderly and disorderly aerodynamics and thermodynamics phenomena. Besides, supersonic combustion includes high velocity motion and coupling processes between flow and combustion, the perfect numerical simulations of actual supersonic flow and combustion processes are rather difficult[21]. With this understanding, one-dimensional method based on actual experimental conclusion will be desirable for distributed parameter control. First, one-dimensional distribution can describe the important characteristics of scramjet engines avoiding the influence of unimportant information[22]. Although there exist multi-scale turbulence and local three-dimensional effects, the macroscopical mixture, diffusion and pressure distribution can not be substantively affected. Secondly, there are lots of experimental data in ground tests to be used such as pressure, temperature and stagnation parameters. These experimental data have contained the main information such as the shape of shock system, separation zones, combustion efficiency and thrust level, which can be used to conclude and describe the one-dimensional distribution of scramjet engines. Thirdly, control methods based on one-dimensional models have been applied to some distributed parameter plants. Finally, as to the errors and uncertainties of one-dimensional simplifications, there are in the control theory the robust control methods to deal with these problems[23]. These mean that one space dimension is necessary and feasible.

The third choice is two or three space dimension. It is a difficult choice because of the complex flow and combustion processes of scramjet engines and the insufficient supports in control theories for the present. However, we may use it in the future.

4.0 REASONABLE FREQUENCY-DOMAIN SIMPLIFICATION FOR DISTRIBUTED PARAMETER CONTROL: STEADY-STATE CONTROL PROCEDURE FOR SCRAMJET ENGINES

Scramjet engines operate under steady state and transient conditions. At each steady state there exists equilibrium condition for engine temperature, pressure and Mach number. Change in fuel injection or flight Mach number will result in transients and thereafter establishment of new steady state conditions. Transient processes are the important characteristics of a scramjet engine and it determines its dynamic properties as a controlled plant. But because scramjet engines are complex flow and combustion systems, their dynamic properties are extremely complicated[24]. It is difficult to set up a

https://doi.org/10.1017/S0001924000001901 Published online by Cambridge University Press

practicable distributed parameter dynamic model. Therefore reasonable simplifications are of great significance. The resulting simplification may be very powerful leading to solutions of the desired performance. To acquire the simplifications, we analyse the dynamic mechanism of the physical system. The main dynamic processes of a scramjet engine include shock dynamics, perturbation waves transmission, flow separation dynamics, ignition delay and combustion oscillation.

4.1 Main dynamics of scramjet engines

4.1.1 Shock dynamics

A shock can be thought as a discontinuous interface that divides the airflow into two sections: high-density and low-density. The motion of the interface changes the mass, momentum, and energy of the flow passing through it. When the shock is finally stable in a new position, the flow is brought into a new balance. In the process, the perturbation energy is partially dissipated by shock compression and viscosity, and the rest of the energy is deposited into the flow passing through the shock. Therefore, it is evident that the fundamental mechanism of the dynamics of shock motion is the energy storage effects of the flow passing through the shock. According to Refs 15 and 25, under certain inlet geometry and operation conditions, the calculated bandwidth of a shock is above 20Hz.

4.1.2 Perturbation waves transmission

Atmospheric disturbances and downstream boundary condition in general result in both acoustic and entropy disturbances. These disturbance components are assumed to travel through the inlet in the form of characteristic waves. Using the linearisation analysis for a quasi-one-dimensional flow through the inlet, these waves can be expressed as a superposition of fast acoustic waves J^+ traveling with a speed of $u+a$, slow acoustic waves J^- traveling with a speed of $u–a$, and entropy waves E traveling with speed u. The propagation time τ_p for each wave type to travel from x_i to x_j is given by

$$\tau_p^{\pm} = \int_{x_i}^{x_j} \frac{1}{a} \frac{1}{\mathrm{M} \pm 1} \mathrm{d}x \qquad \ldots (4)$$

$$\tau_p^{E} = \int_{x_i}^{x_j} \frac{1}{a\mathrm{M}} \mathrm{d}x \qquad \ldots (5)$$

These time constants are expressed in terms of its thermodynamic parameter. It is seen that with increase in speed these time constants tend to become smaller. Numerical results show that the bandwidth of the perturbation wave transmission is around 20Hz[26].

4.1.3 Flow separation dynamics

Flow separation strongly depends on flow governing parameter (e.g. Reynolds number, geometry of surface, upstream and downstream conditions). The condition under which flow separation occurs with dynamic consequences is one of the fundamental areas of interest in fluid mechanics research. Although the mechanisms underlying flow separation dynamics are not fully understood, there have been extensive experimental and numerical validations. Experimental results show that the first-order response frequency of separation dynamics is around 50Hz[27].

4.1.4 Ignition delay and combustion oscillation

Ignition delay in scramjet engines is a short period and the time scale of this period is about $10^{-4}s$ which is similar to the time scale of the supersonic flow in the combustor[28]. Combustion oscillation is generated due to the inherent coupling between several intricate physical phenomena in these processes involving acoustics, thermodynamics, turbulence, and chemical reactions. Energy supplied by the oscillatory combustion processes produce an oscillatory heat release that excites one or more of the natural acoustics modes of the combustor. According to the Rayleigh criterion, if the heat release is in phase with the local pressure fluctuations, the pressure wave associated with the fluctuation will be locally amplified. This acoustic fluctuation can be transmitted inside a combustor module through subsonic wall boundary layers, mixing layers and recirculation zones. For scramjet engines, bluff bodies, rearward facing steps and cavities are generally used as flame holders. For these types of configurations, the origin of combustion oscillation is attributed to vortex roll-up in the recirculation region. Combustion oscillation in a scramjet engine is commonly characterised by high-frequency processes where the first-order response frequency is around 100Hz[29].

4.2 Reasonable frequency-domain simplification

As discussed above, the dynamics of scramjet engines can be interpreted as a high-frequency dynamics exceeding 20Hz, which is determined by the character time of the aerodynamic and thermodynamic processes of a scramjet engine. However, fuel supply system (including fuel pump, valve and fuel injection system) can not generally respond at such a rapid speed because of components' inertia and bandwidth restriction of control system. The response frequency of the common used fuel supply system is around 5Hz. This means that the dynamics of the fuel supply system becomes the dominant dynamics in the control system of scramjet engines, the flow and combustion dynamics, however, become the subordinate dynamics. With this considering, the dynamics of scramjet engines can be regarded as unmodelled dynamics and be neglected in the whole control system based on the frequency-domain simplification theory. Therefore, we can transform the complex dynamic control problem into a simplified one-dimensional steady-state control problem from a viewpoint of frequency-domain simplification.

5.0 INTRODUCTION OF SHAPE CONTROL THEORY

After determining the space dimension and frequency-domain width, we shall next study the concrete control method. Although due to the efforts of more than 50 years research by many well-known mathematicians and scientists, the mathematical theory for distributed parameter control systems have been well-established. But until recently the classic control tools for distributed parameter systems still rely on such complex mathematical techniques as fourier transforms, semi-group theory, sobolev spaces, etc[30]. The mathematical techniques of the distributed parameter systems have been building since the 1950s on the basis of analytical theory of linear/nonlinear partial differential equations[31,32]. However, development during the last decades has shown serious limitations of these analytical methods, especially in evaluation of the dynamics of complex technological objects[33]. Therefore, in practical applications, some simplified optimisation techniques, such as shape control techniques, are preferred for controlling such systems.

Shape control theory derives from structure optimisation techniques involving manipulating the structure's shape to conform to a desired shape specified by the designers. The true shape control problem is a type of inverse problem with no explicit solutions. The core of shape control is to minimise the objective function usually defined as the squared difference of displacements between the desired and the actual shape. The most common approach to a shape control problem for a system governed by partial differential

https://doi.org/10.1017/S0001924000001901 Published online by Cambridge University Press

equations is to see the problem as a constrained nonlinear optimisation problem solved by the usual iterative methods of nonlinear optimisation, such as Newton or quasi-Newton methods. The method uses an objective function evaluation in the nonlinear optimisation procedure, and the evaluation of the gradient or Hessian of the objective function involves the solution of sensitivity equations for the partial differential equations considered. The notion of shape control was introduced into the journal literature through a contribution by Haftka and Adelman[34]. These authors presented the conception in particular regarding the shape control of space antenna, reflectors etc so as to minimise the overall distortion of large space structures from their original shape. Applications range from controlling the shape of aerodynamic surfaces such as an aerofoil to large flexible space structures. Techniques of using shape control for smart structures were implemented by Balakrishnan[35] and Tan[36]. Agrawal and Treanor[37] employed the shape control algorithm to find the optimal actuator locations and voltages. Recently, Chee *et al*[38]. considered more general error functions including curvatures and slopes and presented procedures to find the optimal voltage distribution in static shape control of smart plates based on numerical optimisation methods. Reference 39 deals with shape control by applied temperature. Murozono and Sumi[40] studied the active vibration control of a flexible cantilever beam by applying a transient thermal bending moment so that active control of the first bending mode is realised. Hsu *et al*[41] studied shape control of composite plates by bonded actuators with a high performance configuration. Moreover, applications of optimal shape theory in fluid mechanics include drag reduction[42], optimal sensor/actuator placement[43], airfoil design[44,45] and the design of wind tunnel elements[46]. However, owing to the complexity of the system and the fact that both measurement and control technology are not perfect enough, in current practice, almost no work is undertaken in systematically studying the problem of shape control from the point of view of control theory. This means the theory is still developing and will continue to evolve over a long period of time.

6.0 STEADY-STATE SHAPE CONTROL ARITHMETIC

Shape control of a scramjet engine is to minimize the objective function defined as the squared difference of displacements between the desired shape (Mach number or pressure distribution along the flow direction) and the feedback shape.

6.1 Problem formulation

Control variables of the scramjet engine control system are the fuel flow rates in different fuel injections, which can be substituted by the equivalent variables: stagnation temperature rise ratio $\tau = [\tau_1, \tau_2, ..., \tau_m]$, where the subscript m denotes the number of fuel injections. The controlled variables are the Mach number distribution (or the pressure distribution). Then the objective function is written as

$$J(\tau) = \frac{1}{2}\int_{x_1}^{x_2}\left[\mathrm{M}(x,\tau) - \mathrm{M}_t(x)\right]^2 \mathrm{d}x \qquad \ldots (6)$$

where $\mathrm{M}_t(x)$ is the target shape, and $\mathrm{M}(x,\tau)$ is the feedback shape. Shape control problem is an inverse design problem and can be formulated as finding an optimal control variable τ^* to minimise this objective function. That is

$$J(\tau^*) \le J(\tau) = \frac{1}{2}\int_{x_1}^{x_2}\left[\mathrm{M}(x,\tau) - \mathrm{M}_t(x)\right]^2 \mathrm{d}x \qquad \ldots (7)$$

Using gradient-based methods to solve the shape optimisation problems, one needs the gradient

$$\nabla J(\tau_i) = \int_{x_1}^{x_2}\left[\mathrm{M}(x,\tau) - \mathrm{M}_t(x)\right]\frac{\partial}{\partial \tau_i}\mathrm{M}(x,\tau)\mathrm{d}x \qquad \ldots (8)$$

Note that the gradient involves both the state and the partial derivative of the state with respect to the control variable. This term is referred to as the sensitivity; henceforth, we use the following notation to denote the sensitivity

$$S(x,\tau_i) = \frac{\partial}{\partial \tau_i}\mathrm{M}(x,\tau) \qquad \ldots (9)$$

In order to evaluate the objective function, the state $\mathrm{M}(x,\tau)$ must be computed. Hence the only additional work required for gradient evaluation is the computation of the sensitivity and forming the vector product in Equation (8). The gradient $\nabla J(\tau_i)$ can be calculated by computing the state and the sensitivity and then forming the inner product of the difference $[\mathrm{M}(x,\tau) - \mathrm{M}_t(x)]$ with the sensitivity.

6.2 One-dimensional model

To give a primary proof on the idea of shape control for scramjet engines, we choose the classic one-dimensional model of an axisymmetric, wall-injection scramjet engine[47,48] as the shape control model. In the model, such physical phenomenon on inlet-combustor interaction as flow separation, shock trains and constant pressure heating are considered, and the generalised one-dimensional flow equation is shown in Equation (3).

L'Hospital's rule can be used to evaluate Equation (3) at the critical point x^*

$$\left(\frac{\mathrm{dM}}{\mathrm{d}x}\right)_* = \frac{1}{4}\left\{-\Omega \pm \sqrt{\Omega^2 - 4\Psi}\right\} \qquad \ldots (10)$$

where

$$\Omega \equiv k\left(\frac{1}{A_c}\frac{\mathrm{d}A_c}{\mathrm{d}x}\right)_* \qquad \ldots (11)$$

$$\Psi \equiv (k-1)\left(\frac{1}{A_c}\frac{\mathrm{d}A_c}{\mathrm{d}x}\right)_*^2 - (1+k)\left(\frac{1}{A_c}\frac{\mathrm{d}^2A_c}{\mathrm{d}x^2}\right)_* + \frac{(1+k)^2}{2}\left(\frac{1}{T_t}\frac{\mathrm{d}^2T_t}{\mathrm{d}x^2}\right)_* \qquad \ldots (12)$$

and the position of the critical point x^* is determined by

$$-\left(\frac{1}{A_c}\frac{\mathrm{d}A_c}{\mathrm{d}x}\right) + \frac{(1+k)}{2}\left(\frac{1}{T_t}\frac{\mathrm{d}T_t}{\mathrm{d}x}\right) = 0 \qquad \ldots (13)$$

6.3 Sensitivity equation

Sensitivities are needed in a gradient-based optimisation process in order to provide the gradients of the objective function. By the differential of Equation (3), we obtain the sensitivity equation

$$\frac{\mathrm{d}}{\mathrm{d}x}S(x,\tau_i) = \left[-N_1\left(\frac{1}{A_c}\frac{\mathrm{d}A_c}{\mathrm{d}x}\right) + N_2\left(\frac{1}{T_t}\frac{\mathrm{d}T_t}{\mathrm{d}x}\right)\right]S(x,\tau_i) + N_3\frac{\partial}{\partial \tau_i}\left(\frac{1}{T_t}\frac{\mathrm{d}T_t}{\mathrm{d}x}\right) \qquad \ldots (14)$$

where

$$N_1 = \frac{2 + (3k-1)\mathrm{M}^2 - (k-1)\mathrm{M}^4}{2(\mathrm{M}^2-1)^2} \qquad \ldots (15)$$

$$N_2 = \frac{2 + (9k-1)\mathrm{M}^2 + (5k^2-8k+1)\mathrm{M}^4 - 3k(k-1)\mathrm{M}^6}{4(\mathrm{M}^2-1)^2} \qquad \ldots (16)$$

$$N_3 = \mathrm{M}\left(\frac{1 + (k-1)\mathrm{M}^2/2}{1-\mathrm{M}^2}\right)\left(\frac{1+k\mathrm{M}^2}{2}\right) \qquad \ldots (17)$$

https://doi.org/10.1017/S0001924000001901 Published online by Cambridge University Press

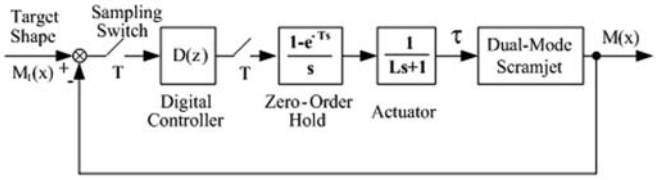


Figure 1. Frame of the shape control system for scramjet engines.

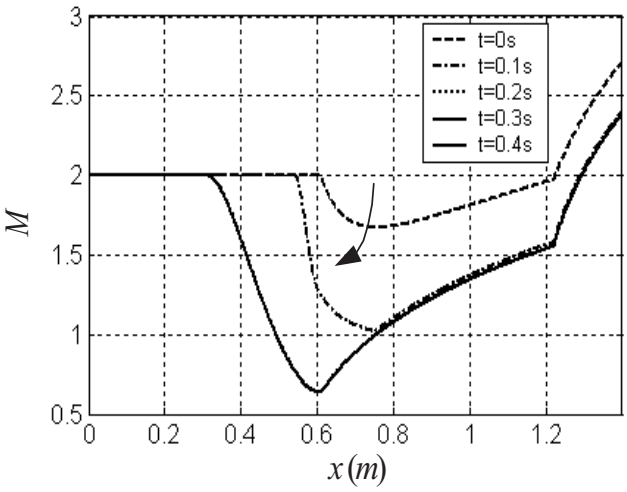


Figure 2. Combustion mode transition process by shape control procedure.

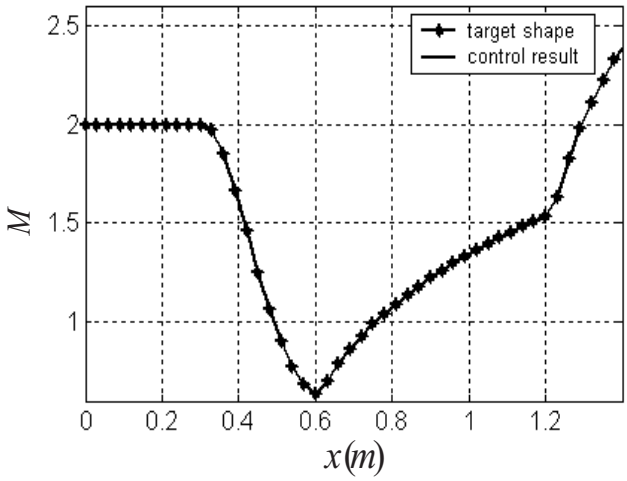


Figure 3. Comparison between the control result and the target mode.

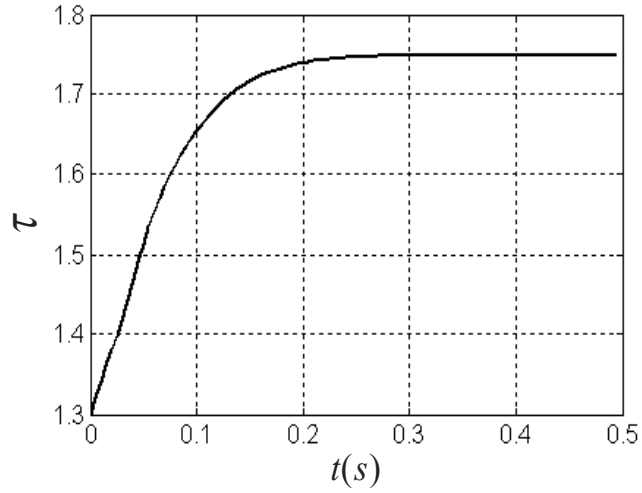


Figure 4. Change of control variable with time.

It is important to observe that Equations (3) and (14) are weakly coupled in the sense that Equation (14) does not feed back into Equation (3), which reduces the calculation difficulty. However, there is a marked difficulty in calculating the sensitivity equation involving singular problem about the critical point, where the denominator $(M^2 - 1)^2$ equals zero. The singular problem will introduce high initial value error and need new solution method in Ref. 49.

6.4 Gauss–Newton optimisation scheme

Gradient-based shape control procedure is a nonlinear optimisation problem and is computationally very expensive usually involving sensitivity function, gradient and Hessian evaluation. Gauss-Newton optimisation scheme is an efficient method for computing the nonlinear optimisation problem. The basis of the optimisation scheme is to approximate Hessian by neglecting the term that involves the second derivative of the residuals. Accordingly, we get

$$\tau_{k+1}^{i} - \tau_{k}^{i} = -\left[\int_{x_1}^{x_2} S(x,\tau_k^i)\mathrm{d}x\right]^{-1} \int_{x_1}^{x_2} [\mathrm{M}(x,\tau_k) - \mathrm{M}_t(x)] S(x,\tau_k^i)\mathrm{d}x \quad \ldots (18)$$

According to the above analysis, we give the basic frame of the shape control system for scramjet engines in Fig. 1 including digital controller, zero-order hold, actuator and control plant.

6.5 A simulation example

The number of fuel injections is currently considered as one. The inertia time constant L of the fuel supply system is set by 0·05 rad/s, and the sampling time T set by 0·005s. The initial shape of Mach number distribution corresponds to the curve marked by '- - -' in Fig. 2, when the scramjet engine operates in the scramjet mode with shock-free isolator and the initial stagnation temperature rise ratio equals to 1·3. The target shape corresponds to the curve marked by "—" in Fig. 3 when the scramjet engine operates in the ramjet mode and the appointed stagnation temperature rise ratio τ^* equals 1·75. Figure 2 shows the mode transition process from the scramjet mode with shock-free isolator to the scramjet mode with oblique shock train and finally to the ramjet mode by the shape control procedures. Figure 3 shows the comparison between the control result and the target shape. Figure 4 shows the changes of objective function and control variable with time respectively. The target shape corresponds to the stagnation temperature rise ratio τ^* of 1·75. According to the simulation result, when t = 0·2s, τ = 1·7341, and the corresponding error is 0·90%; when t = 0·3s, τ = 1·74741, and the corresponding error is 0·14%. Therefore, the shape control system is of high steady accuracy, also with high dynamic performance.

https://doi.org/10.1017/S0001924000001901 Published online by Cambridge University Press

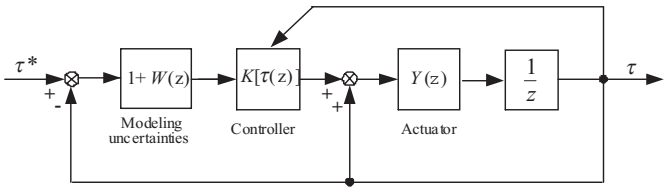


Figure 5. Shape control system by z-transformation.

7.0 A DEMONSTRATION OF THE STEADY-STATE SHAPE CONTROL PROCEDURE

The dynamics of scramjet engines have been regarded as unmodelled dynamics and neglected in the control system design by frequency limitation. Therefore, an important issue should be concerned about the robust stability of the system considering the unmodelled dynamics. In the following section, the robust stability of the shape control system will be demonstrated.

Shape control is a kind of distributed parameter control procedure, and the corresponding robust stability analysis is rather difficult. With this considering, the robust stability analysis is done by transforming the distributed parameter control system into an approximate lumped parameter control system. To do it, the problem on nonlinear transformation between shape and control variable must be solved. Considering the unmodelled dynamics, the shape control procedure can be described as

$$\tau_{k+1} = \left\{\tau_k + H_k S_k^T(x,\tau_k)\left[\mathrm{M}^*(x,\tau^*) - \mathrm{M}_k(x,\tau_k)\right][1+W_k]\right\}Y_k \quad \ldots (19)$$

where Y_h is the dynamics of the actuator, and W_h is the unmodelled dynamics. Because there exists distributed parameter variable in the Equation (19), it is difficult to analyse the robust stability directly. The distributed parameter variable needs to be transformed into lumped parameter variable, that is

$$\mathrm{M}^*(x,\tau^*) - \mathrm{M}_k(x,\tau_k) = \tilde{S}_k(x,\tau_k)(\tau^* - \tau_k) \quad \ldots (20)$$

where $T_{k+n} = \tau^*$, and $\tilde{S}_k(x,\tau_k)$ is defined as an average sensitivity function

$$\tilde{S}_k(x,\tau_k) = E\left(\int_{\tau_k}^{\tau^*} S(x,\tau)\mathrm{d}\tau\right) \cong \frac{1}{n}\sum_{i=k}^{k+n} S_i(x,\tau_i) \quad \ldots (21)$$

The introduction of $\tilde{S}_k(x,\tau_k)$ is just applied for analysis by approximation in Equation (21). According to Equations (19)~(21), we get

$$\tau_{k+1} = \left\{\tau_k + H_k S_k^T(x,\tau_k)\tilde{S}_k(x,\tau_k)\left[\tau^* - \tau_k\right][1+W_k]\right\}Y_k \quad \ldots (22)$$

Making z-transformation to Equation (22), we get

$$z\tau(z) = \left\{\tau(z) + K[\tau(z)]\left[\tau^* - \tau(z)\right][1+W(z)]\right\}Y(z) \quad \ldots (23)$$

where

$$K[\tau(z)] = H[\tau(z)]S^T(x,\tau(z))\tilde{S}(x,\tau(z)) \quad \ldots (24)$$

and

$$Y(z) = \frac{1-\exp(-T/L)}{z-\exp(-T/L)} \quad \ldots (25)$$

The sketch map of the shape control system by z-transformation is shown in Fig. 5. Currently, the shape control system is single input-signal output system, and its robust stability can be analysed based on the classic Nyquist stability criteria. According to the criteria, we obtain the open-loop transfer function as

$$1 + K(z)G_0(z)[1+W(z)] \quad \ldots (26)$$

where

$$G_0(z) = \frac{Y(z)}{z - Y(z)} \quad \ldots (27)$$

Using the Nyquist stability criteria, Fig. 6 shows the Nyquist contour of the nominal open-loop shape control system

$$1 + K(z)G_0(z) \quad \ldots (28)$$

From the Nyquist contour, we can see that the critical point (–1, 0j) is not encircled, and the shape control system has no open-loop poles in the right-hand half of the s plane to be stable. Therefore, it may be concluded that the nominal system is unconditionally stable. To know how close to instability the nominal system is, we calculate the gain and phase margins to express the closeness of the locus to the critical point (–1, 0j), and the results are that the gain margin GM (if GM > 0dB, the system is stable) equals to 19·6dB; the phase margin PM (if PM > 0°, the system is stable) equals to 82°. The calculated results mean that the nominal shape control system is of high relative stability. Following this frequency analysis, the close-loop nominal shape control system is simulated and shown in Fig. 7, and the simulation result is consistent with the frequency analysis.

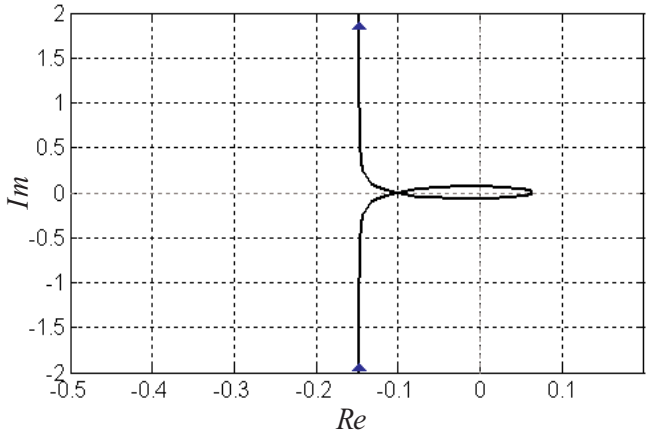


Figure 6. Nyquist chart of the nominal shape control system.

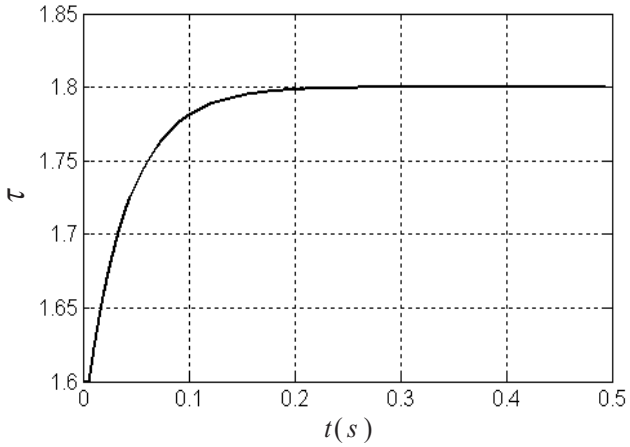


Figure 7. Simulation of the nominal shape control system.

https://doi.org/10.1017/S0001924000001901 Published online by Cambridge University Press

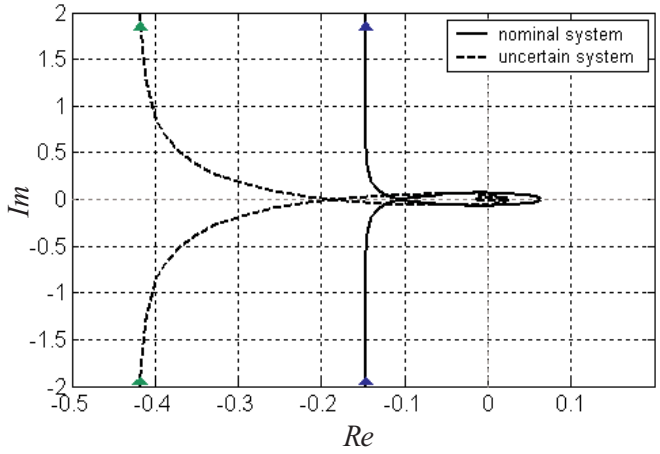


Figure 8. Nyquist chart of the shape control system with one-order model uncertain.

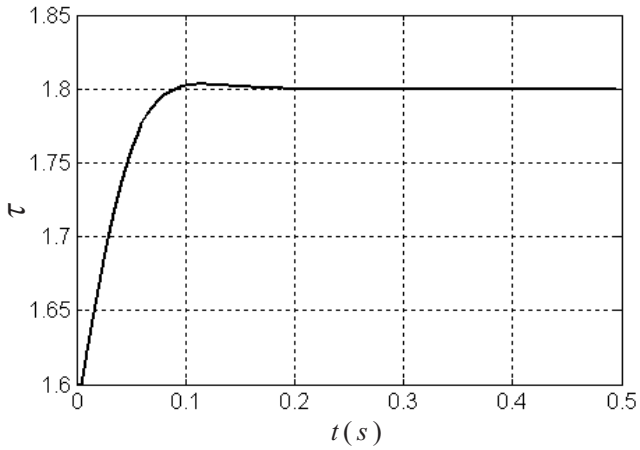


Figure 9. Simulation of the shape control system with one-order model uncertain.

Next we study the robust stability of shape control system with unmodelled dynamics. Firstly, we consider the unmodeled dynamics as one-order system whose z-transfer function is written as

$$W(z)=\frac{1-\exp(-T/L_1)}{z-\exp(-T/L_1)}-1 \qquad \ldots (29)$$

where L_1 is the time constant. Because the model error increases when the bandwidth of the unmodelled dynamics decreases, the lowest bandwidth of the unmodelled dynamics is chosen to validate the robust stability of the shape control system. According to the analysis of the dynamical mechanics of scramjet engines, we choose the possibly lowest bandwidth of the one-order unmodelled dynamics as 10Hz (the corresponding time constant L_1 = 0·0106s). Then the open-loop transfer function of the shape control system with one-order unmodelled dynamics is obtained as

$$1+K(z)G_0(z)\frac{1-\exp(-T/L_1)}{z-\exp(-T/L_1)} \qquad \ldots (30)$$

Using the Nyquist stability criteria, Fig. 8 shows the Nyquist contour of this open-loop shape control system. From the Nyquist contour, we can see that the critical point (–1, 0j) is not encircled which means that the shape control system with two-order unmodelled dynamics is stable. By calculation, the gain margin GM equals to 14·5dB; the phase margin PM equals to 66°, which means the relative stability falls slightly. The corresponding simulation result of the close-loop shape control system is shown in Fig. 9.

Secondly, we consider the unmodelled dynamics as two-order system whose z-transfer function is written as

$$W(z)=\frac{b_1z+b_2}{z^2+a_1z+a_2}-1 \qquad \ldots (31)$$

where

$$a_1=-2\exp(-\xi\omega_0T\sqrt{1-\xi^2})\mathrm{Cos}(\omega_0T\sqrt{1-\xi^2})$$

$$a_2=\left[\exp(-\xi\omega_0T\sqrt{1-\xi^2})\right]^2 \qquad \ldots (32)$$

$$b_1=1-\exp(-\xi\omega_0T\sqrt{1-\xi^2})\left[\mathrm{Cos}(\omega_0T\sqrt{1-\xi^2})+\frac{\xi\omega_0}{\omega_0\sqrt{1-\xi^2}\mathrm{Sin}(\omega_0T\sqrt{1-\xi^2})}\right]$$

$$b_2=\left[\exp(-\xi\omega_0T\sqrt{1-\xi^2})\right]^2+\exp(-\xi\omega_0T\sqrt{1-\xi^2})\left[\frac{\xi\omega_0}{\omega_0\sqrt{1-\xi^2}\mathrm{Sin}(\omega_0T\sqrt{1-\xi^2})}\right.$$

$$\left.-\mathrm{Cos}(\omega_0T\sqrt{1-\xi^2})\right]$$

where ω_0 is the shear frequency, and ξ is the damping coefficient. According to the analysis of the dynamical mechanics of scramjet engines, we choose the possibly lowest shear frequency of the two-order unmodelled dynamics as 100Hz, and damping coefficient as 0·15. Then the open-loop transfer function of the shape control system with two-order unmodelled dynamics is obtained as

$$1+K(z)G_0(z)\frac{b_1z+b_2}{z^2+a_1z+a_2} \qquad \ldots (33)$$

Using the Nyquist stability criteria, Fig. 10 shows the Nyquist contour of this open-loop shape control system. From the Nyquist contour, we can see that the critical point (–1, 0j) is still not encircled which means that the shape control system with one-order unmodelled dynamics is also unconditionally stable. By calculation, the gain margin GM equals to 11·1dB; the phase margin PM equals to 68·7°, and the system's relative stability falls slightly comparing with the nominal shape control system. The corresponding simulation result of the close-loop shape control system is shown in Fig. 11.

As analysed above, the nominal shape control system has good robust stability to the unmodelled dynamics. These results demonstrate the idea of simplification by transforming the complex dynamic control problem into a simplified steady-state control problem from a viewpoint of frequency limitation.

8.0 CONCLUSIONS

First, this paper reveals that distributed parameter control may play a key role in the solution to the essential control problem of scramjet engines, that is, properly regulating heat release profiles and flow parameter distributions can help to decrease the losses of supersonic combustion and shock trains, and better the matching performance among inlet, combustor and nozzle over a wide speed range. Secondly, this paper analyses the space dimension of distributed parameter control and confirms that one-dimensional method based on actual experimental emendation will be desirable for the present technology level. Thirdly, by analysing the dynamic mechanism of the physical system, this paper proposes that the dynamics of

https://doi.org/10.1017/S0001924000001901 Published online by Cambridge University Press

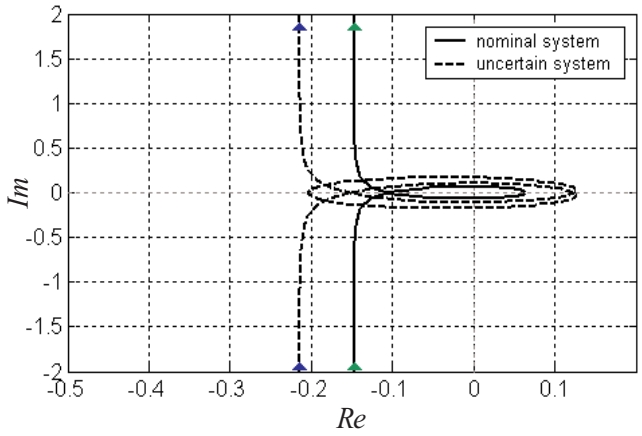


Figure 10. Nyquist chart of the shape control system with two-order model uncertain.

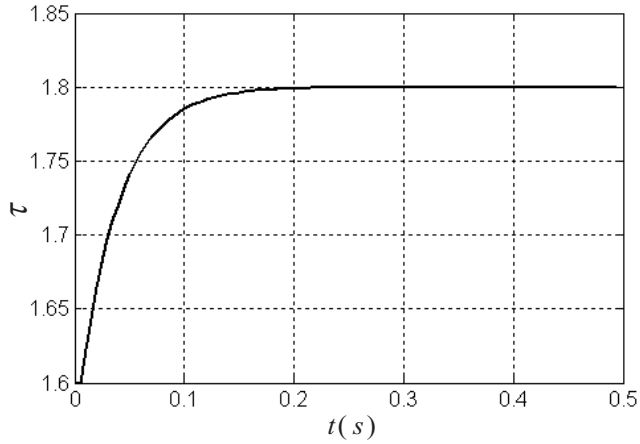


Figure 11. Simulation of the shape control system with two-order model uncertain.

scramjet engines can be regarded as unmodelled dynamics and be neglected in the whole control system based on the frequency-domain simplification theory. Thereby, the complex dynamic control problem can be transformed into a simplified steady-state control problem from a viewpoint of robust control, which makes feasible the distributed parameter control for scramjet engines. Fourthly, a new design method based on shape control theory is put forward to realise the distributed parameter control of scramjet engines, and simulation results show its validities in steady accuracy and dynamic performance. Finally, the idea of steady-state shape control procedure for scramjet engines is demonstrated by the theoretic analysis using the robust stability theories. The control procedure presented in this paper may have a potential use in the other hypersonic propulsion systems.

ACKNOWLEDGMENTS

The authors would like to thank Program for Outstanding Youth Foundation of Heilongjiang Province, China.

REFERENCES

1. HAREFORS, M. Application of control structure design methods to a jet engine, *J Guidance, Control, and Dynamics*, 2001, **24**, (3), pp 510-518.
2. LAWRENCE, D.H., KENNETH, E.R. and EDWARD, G.R. Hyper-X flight engine ground testing for X-43 flight risk reduction, April 2001, AIAA Paper 2001-1809.
3. UMAIR, A., ALI, M. and PADUANO, J.D. Design of a near-isentropic supersonic inlet using active control, *J Propulsion and Power*, 2005, **22**, (2), pp 292-299.
4. YU, G., LI, J.G. and CHANG, X.Y. Fuel injection and flame stabilization in a liquid-kerosene-fueled supersonic combustor, *J Propulsion and Power*, 2003, **19**, (5), pp 885-893.
5. SIEBENHAAR, A. and BULMAN, M. Development and testing of the aerojet strutjet combustor, August 1999, AIAA 99-4868.
6. EDWARD, T.C. Scramjet Engines: The First Forty Years, *J Propulsion and Power*, 2001, **17**, (6), pp 1138-1148.
7. ALI, M., SADRUL, I. and AHMED, S. Mixing and flame holding with air inlet configuration in scramjet combustor, *Int Comm in Heat and Mass Transfer*, 2004, **31**, (8), pp 1187-1198.
8. GRUBER, M.R., DONBAR, J.M. and CARTER, C.D. Mixing and combustion studies using cavity-based flameholders in a supersonic flow, *J Propulsion and Power*, 2004, **20**, (5), pp 769-778.
9. MU, J., REES, D. and LIU, G.P. Advanced controller design for aircraft gas turbine engines, *Control Engineering Practice*, 2005, **13**, (8), pp 1001-1015.
10. TOMIOKA, S., KOBAYASHI, K. and MURAKAMI, A. Distributed fuel injection for performance improvement of staged supersonic combustor, *J Propulsion and Power*, 2005, **21**, (4), pp 760-763.
11. GALLIMORE, S.D., JACOBSEN, L.S. and O'BRIEN, W.F. Operational sensitivities of an integrated scramjet ignition/fuel-injection system, *J Propulsion and Power*, 2003, **19**, (6), pp 183-189.
12. HAREFORS, M. Application of control structure design methods to a jet engine, *J Guidance, Control, and Dynamics*, 2001, **24**, (3), pp 510-518.
13. HASHEM, A.A. and NADA, T.R. Design of turbofan engine controller based on non-linear analysis, *J Eng and Applied Science*, 2002, **48**, (1), pp 137-153.
14. WANG, F., FAN, S.Q. and WU, D. Study of MAPS methods for turbofan engine performance seeking control, *J Aerospace Power*, 2005, **20**, (3), pp 503-507.
15. MACMARTIN, D.G. Dynamics and control of shock motion in a near-isentropic inlet, *J Aircr*, 2004, **41**, (4), pp 846–853.
16. CHRISTIAN, T., LANDRUM, D.B. and YURI, S.C. Ramjet-powered reusable launch vehicle control by sliding modes, *J Guidance, Control, and Dynamics*, 1998, **21**, (3), pp 409-415.
17. HOO, K.A. and ZHENG, D. Low-order control-relevant models for a class of distributed parameter systems, *Chemical Engineering Science*, 2001, **56**, (23), pp 6683-6710.
18. MITANI, T., HIRAIWA, T. and MASUYA, G. Drag and total pressure distributions in scramjet engines at Mach 8 flight, *J Propulsion and Power*, 2002, **18**, (4), pp 953-960.
19. TAKESHI, K. and NOBUO, C. Dual-mode operation in a scramjet combustor, April 2001, AIAA 2001-1816.
20. EMAMI, N.A. and EBERT, J.L. Modeling and control of distributed thermal systems, *IEEE Transactions on Control Systems Technology*, 2003, **11**, (5), pp 668-683.
21. OEVERMANN, M. Numerical investigation of turbulent hydrogen combustion in a scramjet using flamelet modeling, *Aerospace Sci and Tech*, 2000, **4**, (7), pp 463-480.
22. O'BRIEN, T.F., STARKEY, R.P. and LEWIS, M.J. Quasi-one-dimensional high-speed engine model with finite-rate chemistry, *J Propulsion and Power*, 2001, **17**, (6), pp 1366-1374.
23. REINSCHKE, J., CANTONI, M.W. and SMITH, M.C. A robust control framework for linear time-invariant, spatially distributed systems, *SIAM J Control and Optimization*, 2002, **40**, (2), pp 610-627.
24. SAJBEN, M. and SAID, H. Acoustic-wave/ blade-row interactions establish boundary conditions for unsteady inlet flows, *J Propulsion and Power*, 2001, **17**, (5), pp 1090-1099.
25. DAREN, Y., TAO, C. and WEN, B. Equilibrium manifold linearization model for normal shock position control systems, *J Aircr*, 2005, **42**, (5), pp 1344-1347.
26. WILLOH, R.G. A mathematics analysis of supersonic inlet dynamic, August 1968, NASA TND-4969.
27. SAMANTHA, H.F. and DOUGLAS, G.M. Dynamic separation control in a low-speed asymmetric diffuser with varying downsteam boundary condition, August 2003, AIAA 2003-4161.

https://doi.org/10.1017/S0001924000001901 Published online by Cambridge University Press

28. GRUENIG, C. and MAYINGER, F. Supersonic combustion of kerosene/H_2 mixture in a model scramjet combustor, *Combustion Sci and Tech*, 1999, **14**, (6), pp 1-22.
29. MCMANUS, K.R. A review of active control of combustion instabilities, *Prog in Energy and Combustion Sci*, 1993, **19**, (2), pp 1-29.
30. GODASI, S., KARAKAS, A. and PALAZOGLU, A. Control of nonlinear distributed parameter processes using symmetry groups and invariance conditions, *Computers and Chemical Eng*, 2002, **26**, (7), pp 1023-1036.
31. HIRONOYI, AF. Distributed parameter approach to control large space structures, 1995, Proceeding of the 35th Conference on Decision and Control, Kobe, Japan.
32. KARLSSON, N. Optimal nonlinear distributed control of spatially-invariant systems, 2001, Proceeding of the 40th IEEE conference on decision and control, Orlando, Florida.
33. YU, D.R., CUI, T. and BAO, W. Distributed parameter control method for hypersonic jets, *J Aerospace Power*, 2004, **19**, (2), pp 259-264.
34. HAFTKA, R.T. and ADELMAN, H.M. An analytical investigation of shape control of large space structures by applied temperatures, *AIAA J*, 1985, **23**, (45), pp 1-7.
35. BALAKRISHNAN, A.V. Shape control of plates with piezo actuators and collocated position/rate sensors, *Applied Math and Computation*, 1994, **6**, (3), pp 213-234.
36. TAN, Z. Optimal linear quadratic Gaussian digital control of an orbiting tethered antenna/reflector system, *J Guidance, Control and Dynamics*, 1994, **17**, (2), pp 234-241.
37. AGRAWAL, B.N. and TREANOR, K.E. Shape control of a beam using piezoelectric actuators, *Smart Materials and Structures*, 1999, **8**, (6), pp 729-739.
38. CHEE, C., TONG, L.Y. and STEVEN, G.P. Static shape control of composite plates using a slope-displacement-based algorithm, *AIAA J*, 2002, **40**, (8), pp 1611–1618.
39. IRSCHIK, H. and PICHLER, U. Dynamic shape control of solids and structures by thermal expansion strains, *J Thermal Stresses*, 2001, **24**, (3), pp 565-78.
40. MUROZONO, M. and SUMI, S. Active vibration control of a flexible cantilever beam by applying thermal bending moment, *J Intelligent Material and System Structure*, 1994, **5**, (4), pp 21-9.
41. HSU, C.Y., LIN, C.C. and GAUL, L. Shape control of composite plates by bonded actuators with high performance configuration, *J Reinforced Plastics Composition*, 1997, **16**, (18), pp 1692–710.
42. JOSYULA, E., PINNEY, M. and BLAKE, W.B. Applications of a counter flow drag reduction technique in high-speed systems, *J Spacecraft and Rockets*, 2002, **39**, (4), pp 605-614.
43. KIM, S.J. and SONG, K.Y. Active control of sound fields from plates in flow by piezoelectric sensor/actuator, *AIAA J*, 1999, **27**, (10), pp 1180-1186.
44. ELESHAKY, M.E. and BAYSAL, O. Airfoil shape optimization using sensitivity analysis on viscous flow equations, *J Fluids Engineering*, 1993, **115**, (1), pp 75-84.
45. ASHRAFIZADEH, A., RAITHBY, G.D. and STUBLEY, G.D. Direct design of airfoil shape with a prescribed surface pressure, *Numerical Heat Transfer*, 2004, **46**, (6), pp 505-527.
46. COCHRAN, L.S. and HOWELL, J.F. Wind tunnel studies for the aerodynamic shape for Sydney Australia, *J Wind Eng and Industrial Aerodynamics*, 1990, **36**, (2), pp 801-810.
47. HEISER, W. and PRATT, D. Hypersonic airbreathing propulsion, 1994, AIAA, Washington, DC.
48. TIMOTHY, F.O., RYAN, P.S. and MARK, J.L. Quasi-one-dimensional high-speed engine model with finite-rate chemistry, *J Propulsion and Power*, 2001, **17**, (6), pp 1366-1374.
49. CUI, T., YU, D.R. and BAO, W. Solution method for singular initial value problems of one-dimensional steady transonic flow in a dual-mode scramjet, *Chinese J Aeronautics*, 2005, **18**, (2), pp 97-101.

https://doi.org/10.1017/S0001924000001901 Published online by Cambridge University Press